Karlsruhe Institute of Technology

Detection and Characterisation of Microwave Emission of EAS with the CROME Experiment

Felix Werner for the CROME group
Institute for Nuclear Physics, KIT

Motivation: Benefits of microwave detection

- extremely low external noise
- negligible atmospheric attenuation

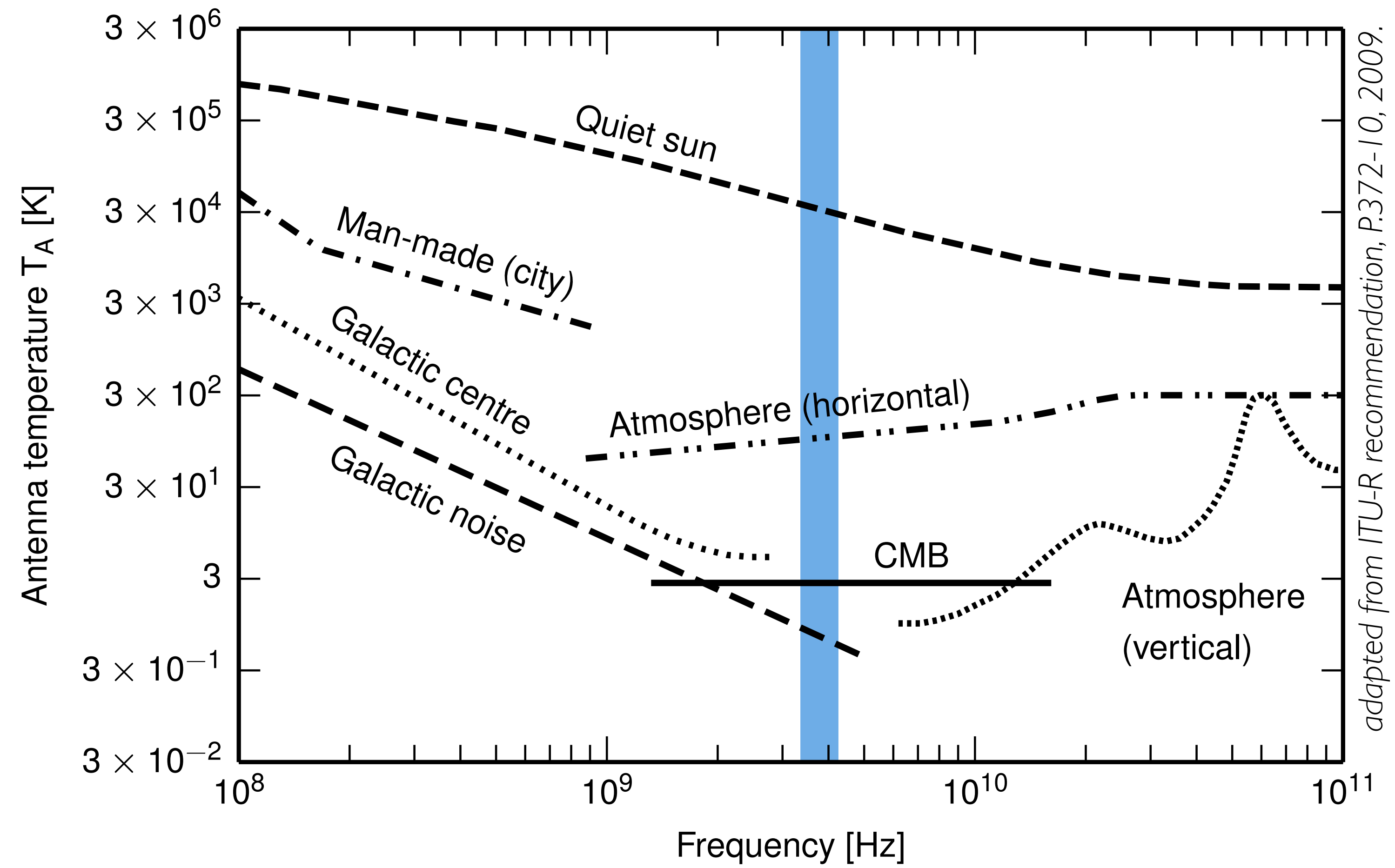

- highly developed off-the-shelf receivers

Low-noise block (LNB)

$T_{sys} \sim 40$ K, $G \sim 65$ dB

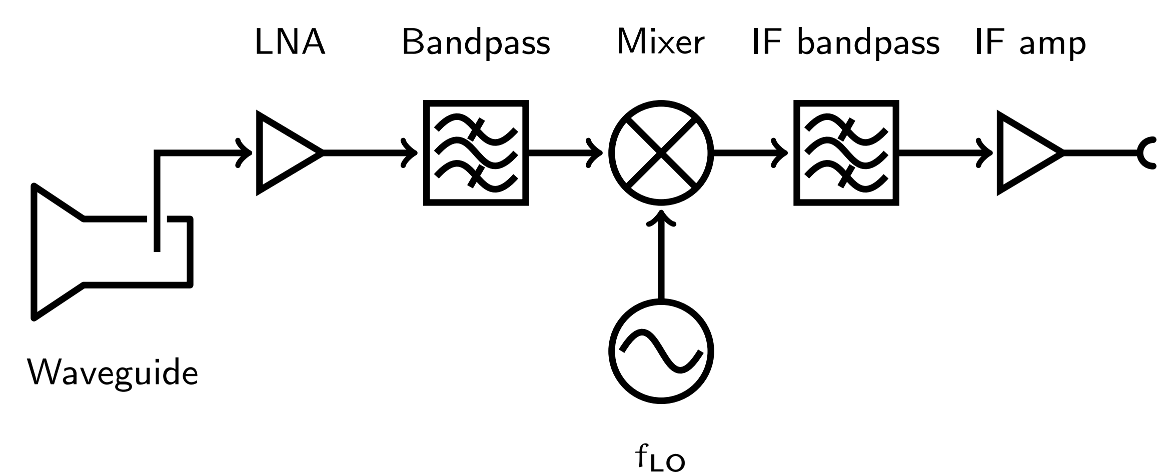

Sources of high-frequency radio emission

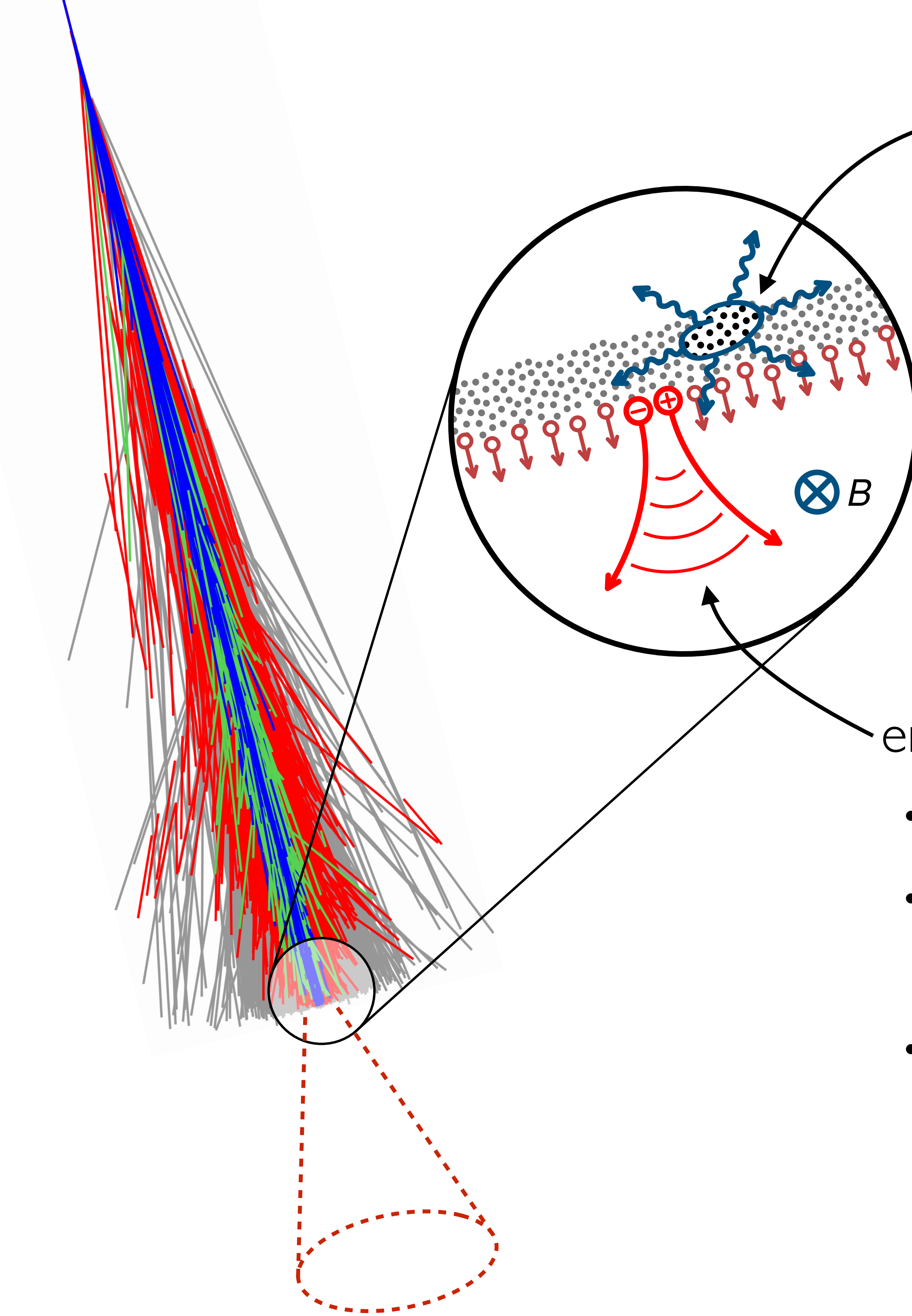

emission of low-energy plasma electrons

- molecular bremsstrahlung
- observed (only) in accelerator experiments
  Gorham et al., Phys. Rev., D78: 032007, 2008.
- unpolarised, **isotropic**, broadband radiation
  - sparked several experimental searches

emission of high-energy charged particles

- mainly geomagnetic & charge-excess effects
- steeply falling frequency spectrum (well-studied for frequencies ≪ 1 GHz)
- time compression near Cherenkov cone
  - highly **forward-beamed** at GHz frequencies

CROME concept

Microwave antenna array **embedded** in KASCADE-Grande:

- antennas pointing vertically
  - time compression of signals leads to natural **increase of SNR**
- detector read-out triggered by high-energy air showers
- signals can be correlated with shower reconstruction from KG
- additional time synchronisation with nearest scintillator station

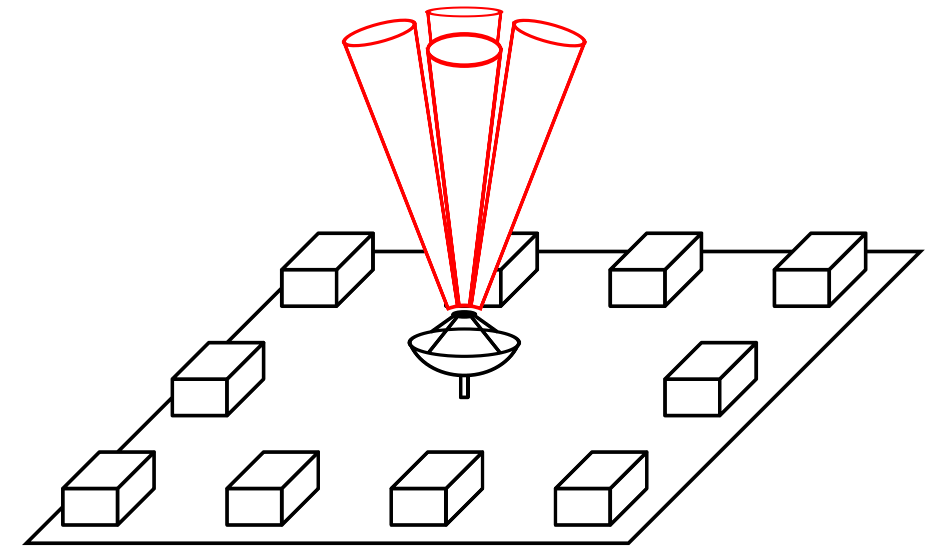

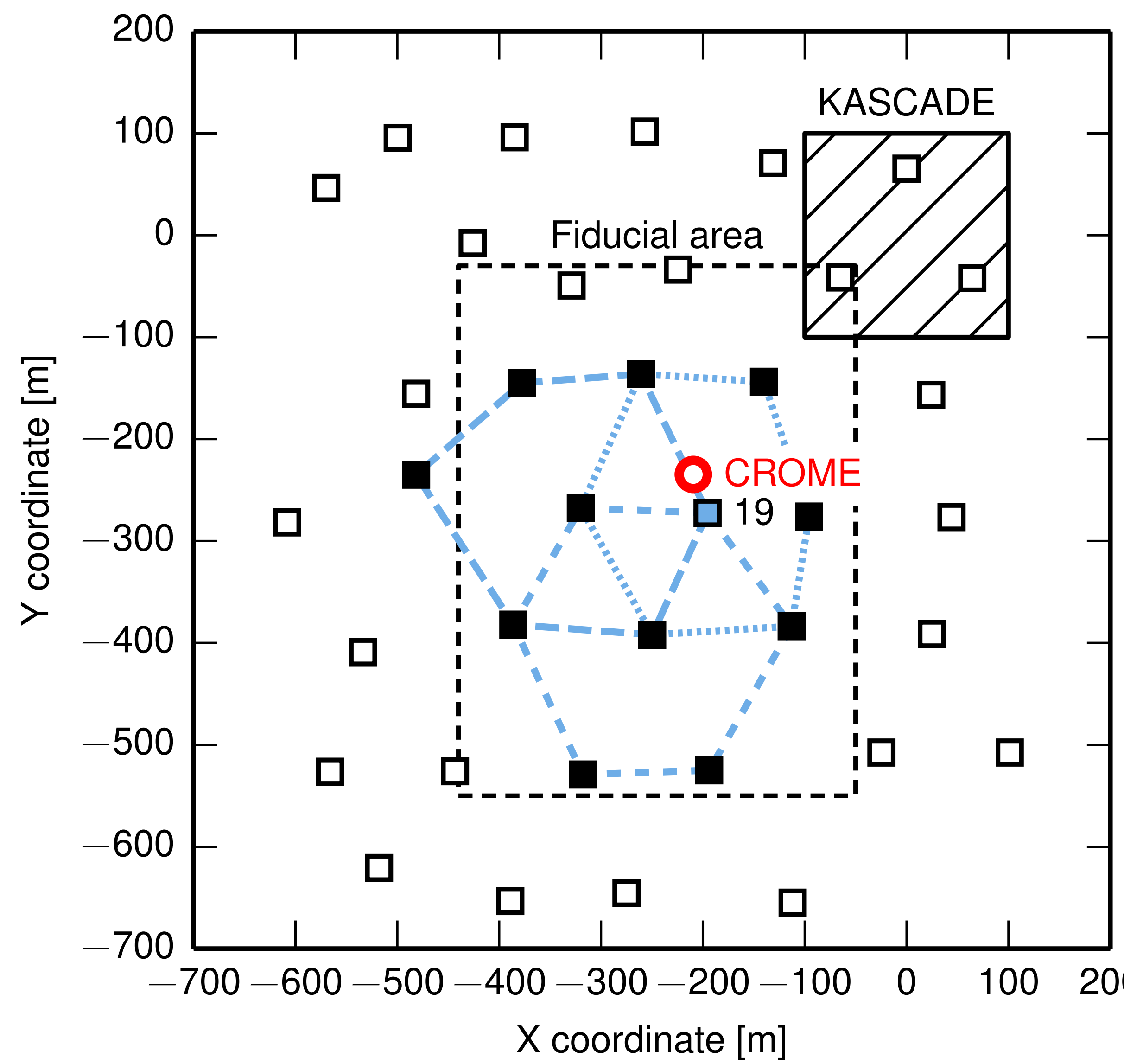

Instrumentation

K band (11 GHz)

June 2010

Instrumentation

L band (1–2 GHz)
see talks by L. Petzold & P. Papenbreer

K band (11 GHz)

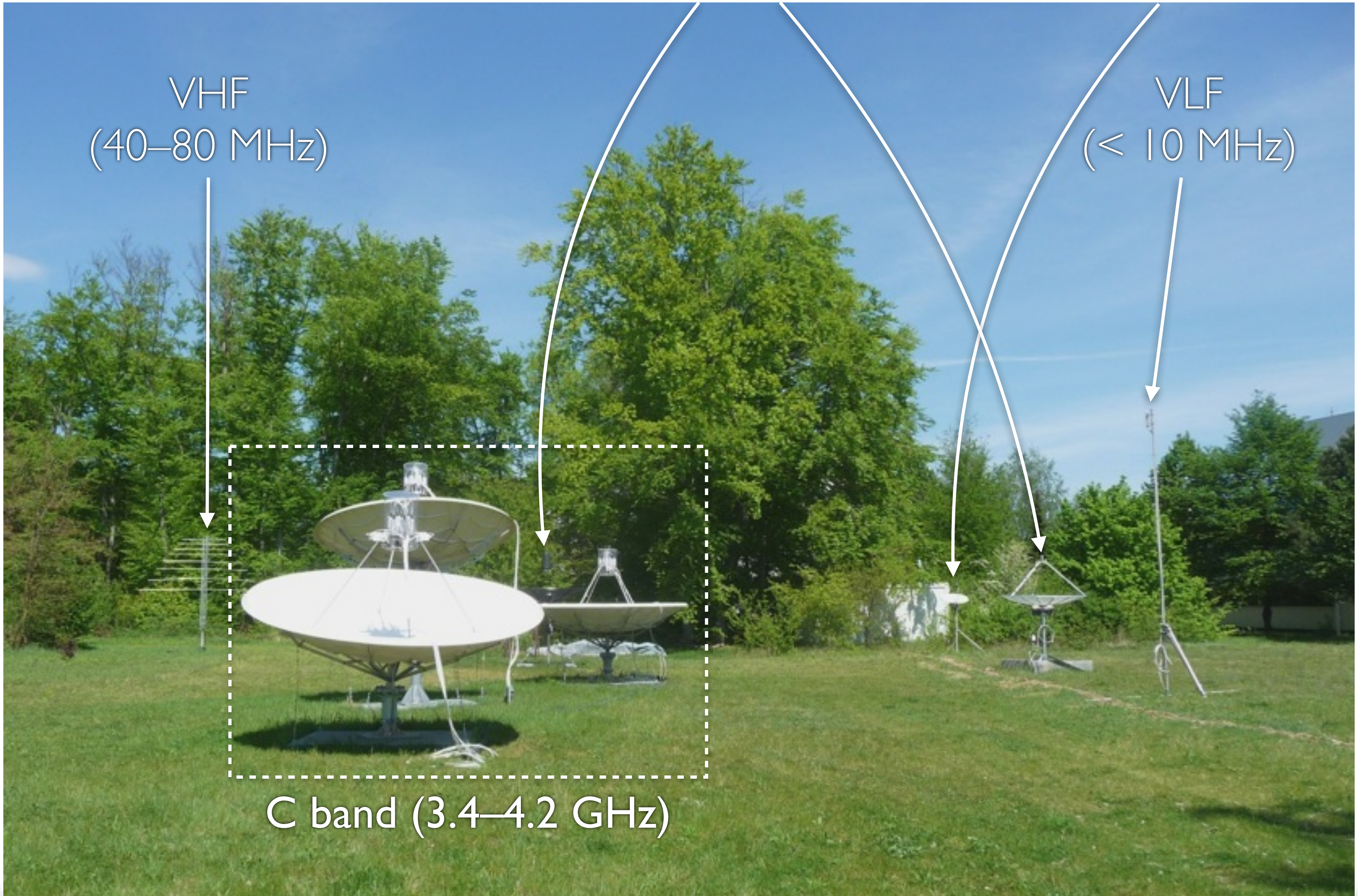

May 2012
shutdown of KG in Nov. 2012

C band setup

- three 3.4 m parabolic reflectors (vertical, 15° to north, 15° to south)
  - 40 dBi gain, 1.7° beam width
- linearly polarised nine-feed cameras equipped with Norsat LNBs (3.4–4.2 GHz)
- corner feeds upgraded for 2nd polarisation

electronics chain

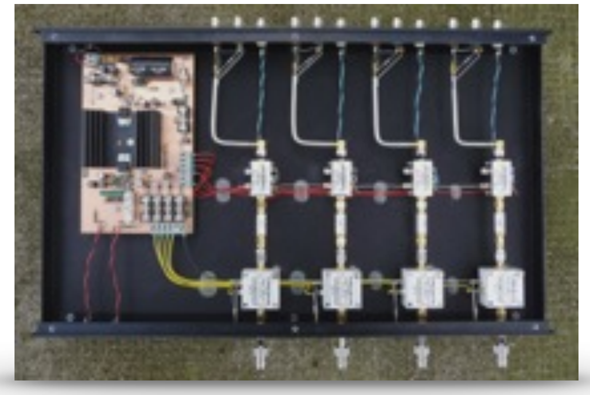

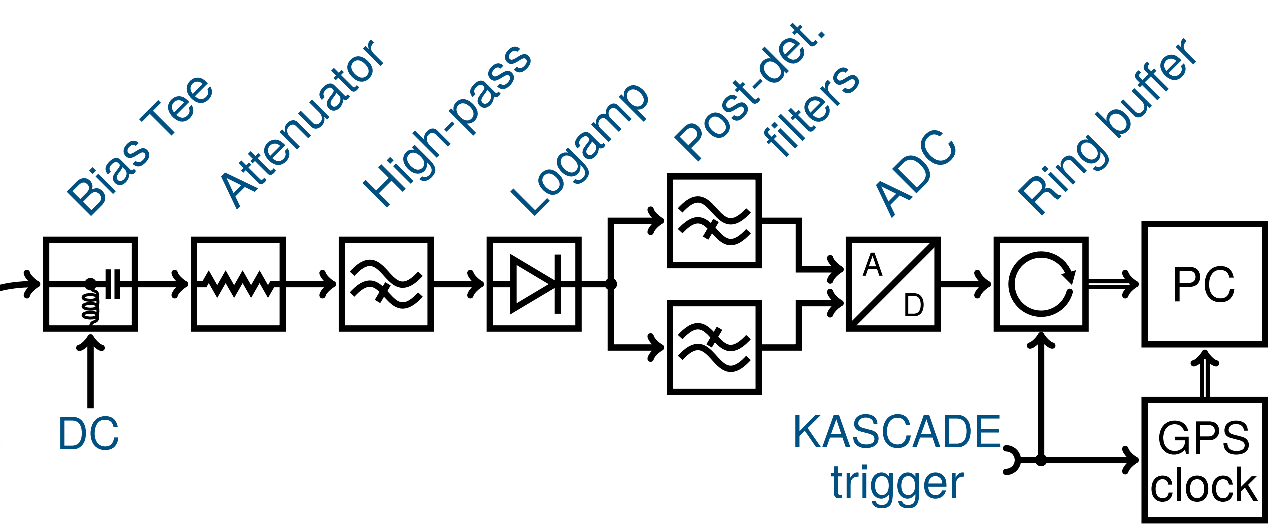

Calibration results

In-situ measurements:

- half-power beam width: 1.7°
- pointing accuracy: 0.1°
- system temperature: 77–87 K

Lab. measurements:

- effective bandwidth: 660 MHz
- end-to-end rise time: 2.7 ns

‣ basis for **end-to-end detector simulation**

flying calibration source

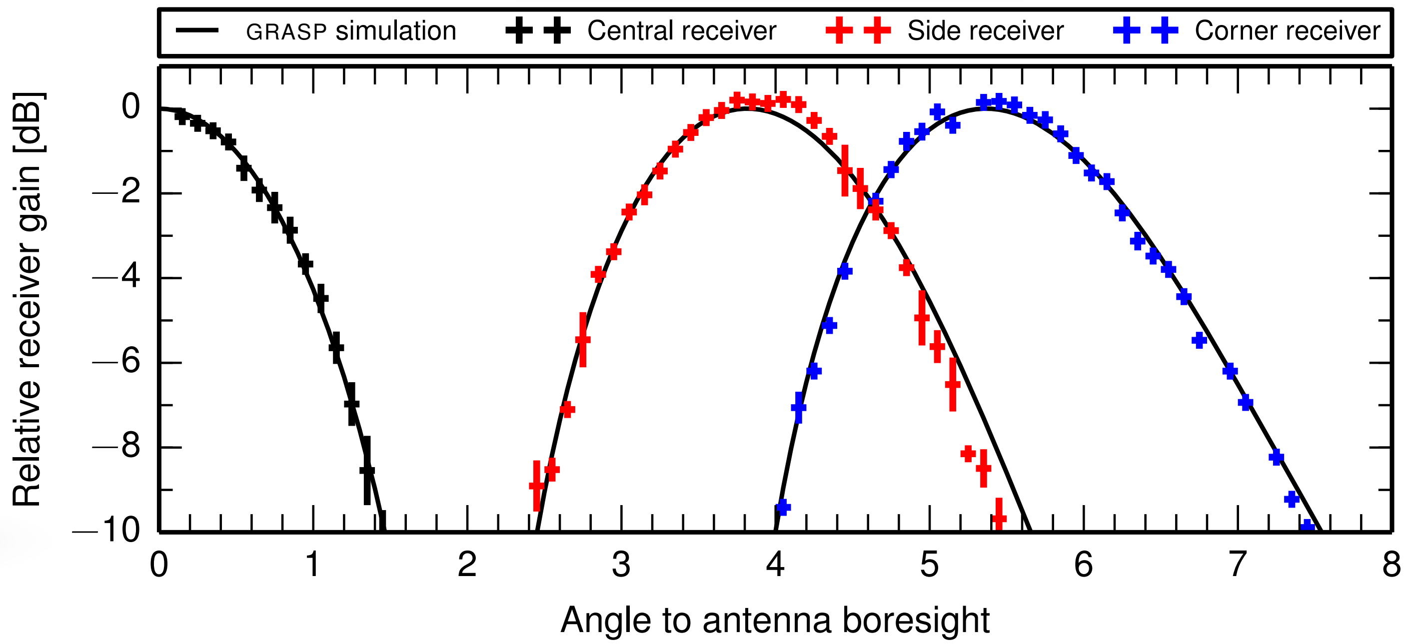

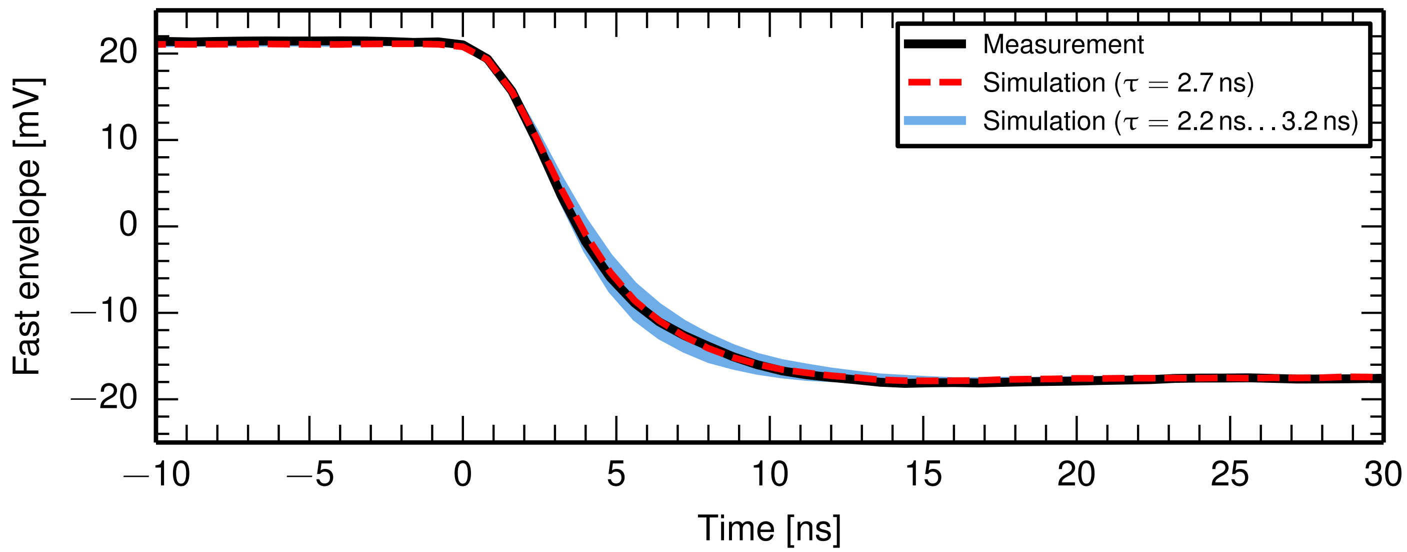

Electronics simulation

Detailed simulation of all components:

- models non-linear response of logamp
- accurately reproduces end-to-end pulse response
- noise distribution well-described by thermal noise

Pulse response

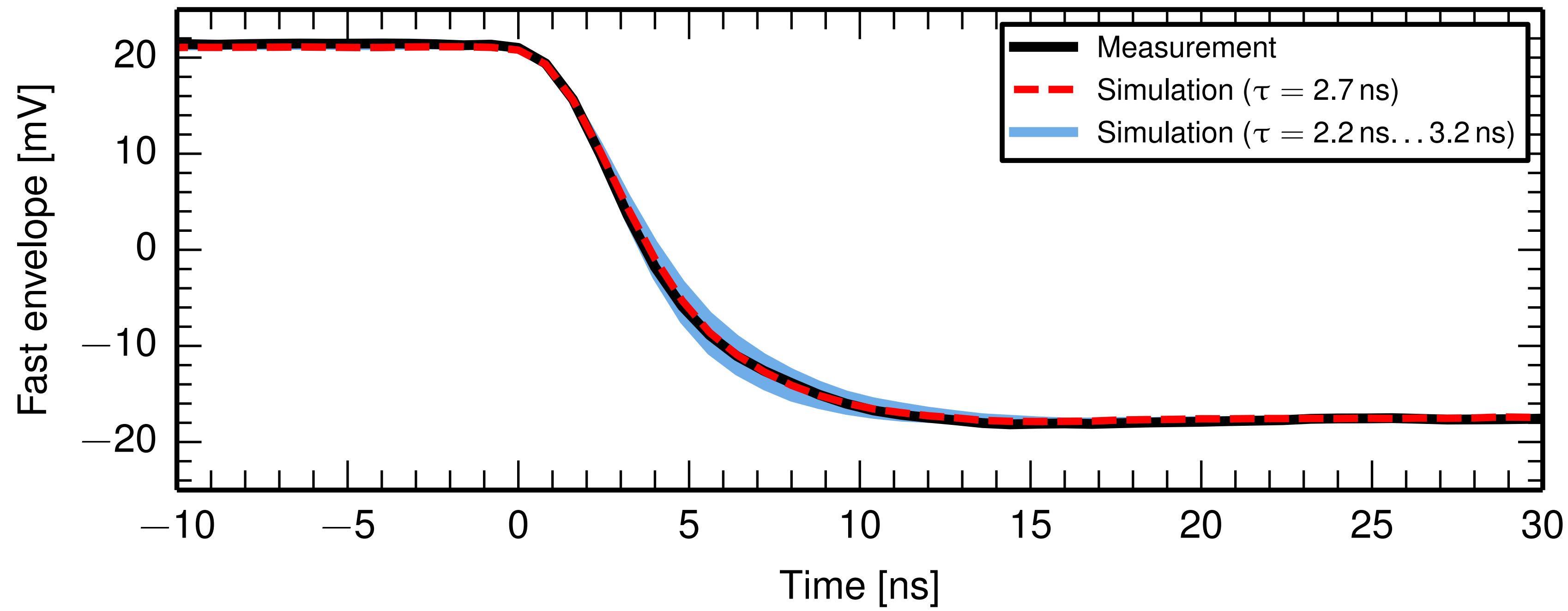

Noise distribution

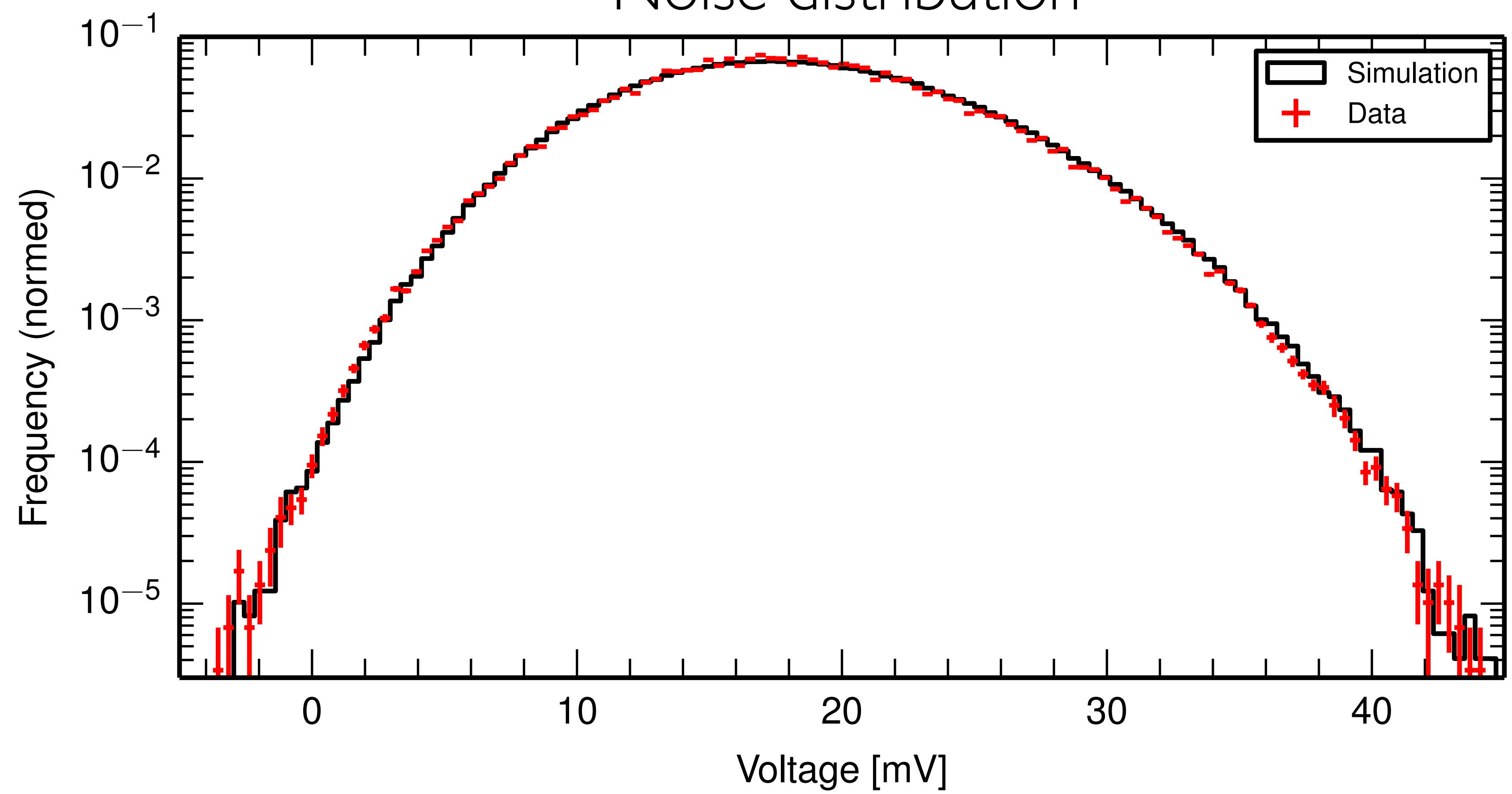

Stability and selection

- temperature-dependent LNB gain leads to daily fluctuations of baseline
- <3% outliers (mostly heavy precipitation and RFI)

Noise level over one month

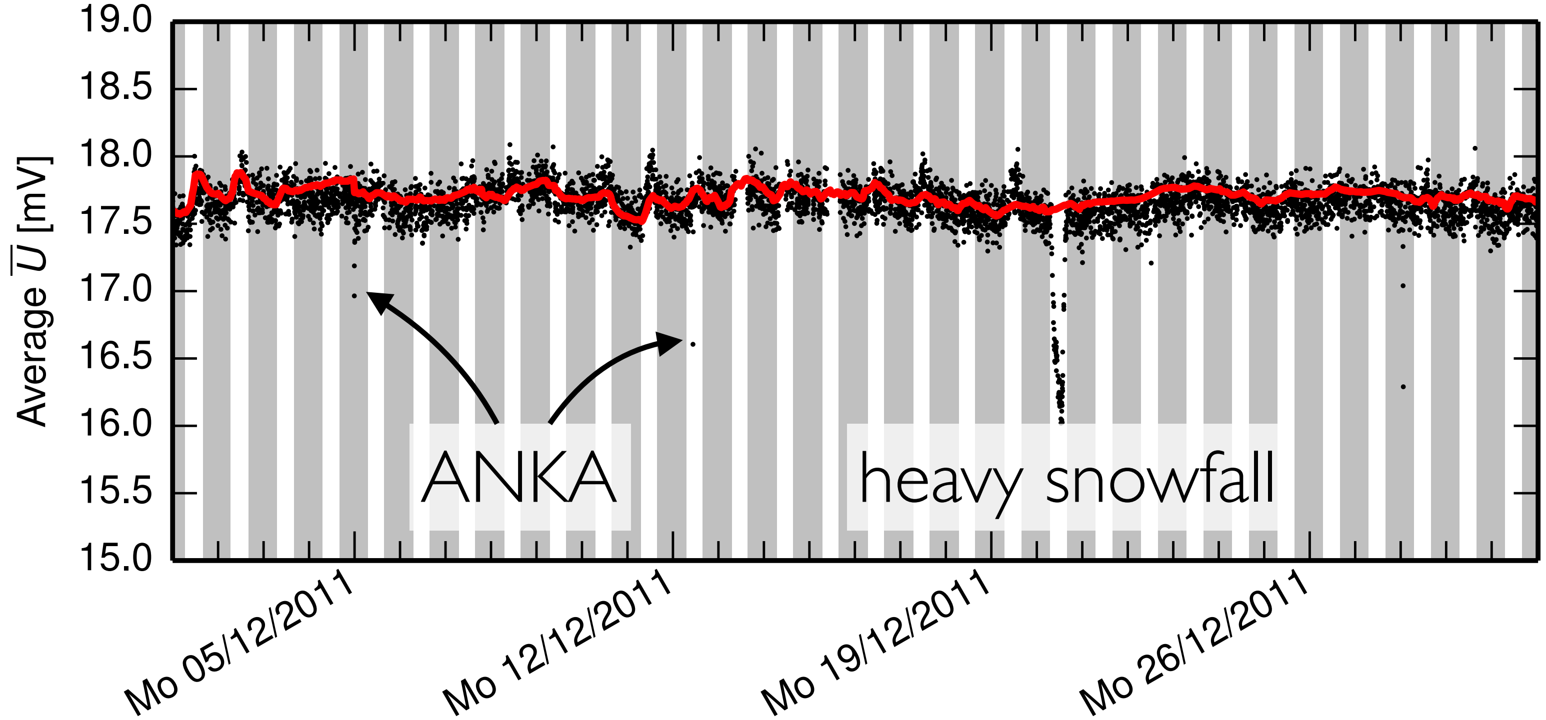

After applying CROME **and** KASCADE-Grande quality cuts:

- baseline fluctuations ΔT_{sys} ~ 12%
- 11,800 hours of common operation
  - single polarisation: 121 sr hours
  - dual polarisation: 20 sr hours
- 15,000 air showers with **E > $10^{16.5}$ eV** and **Θ < 40°**
- **3,700 showers** cross the field of view of at least one receiver

Event selection

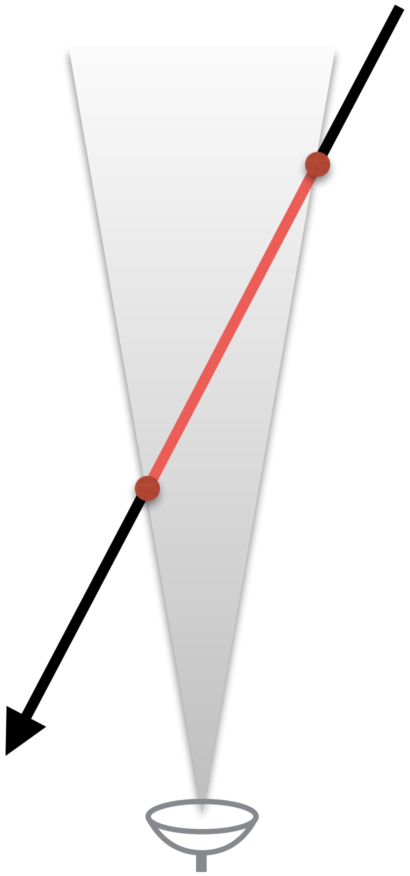

Calculation of expected signal time windows:

- includes uncertainties in electronics (~20 ns) and geometry
- typical widths: 40–60 ns

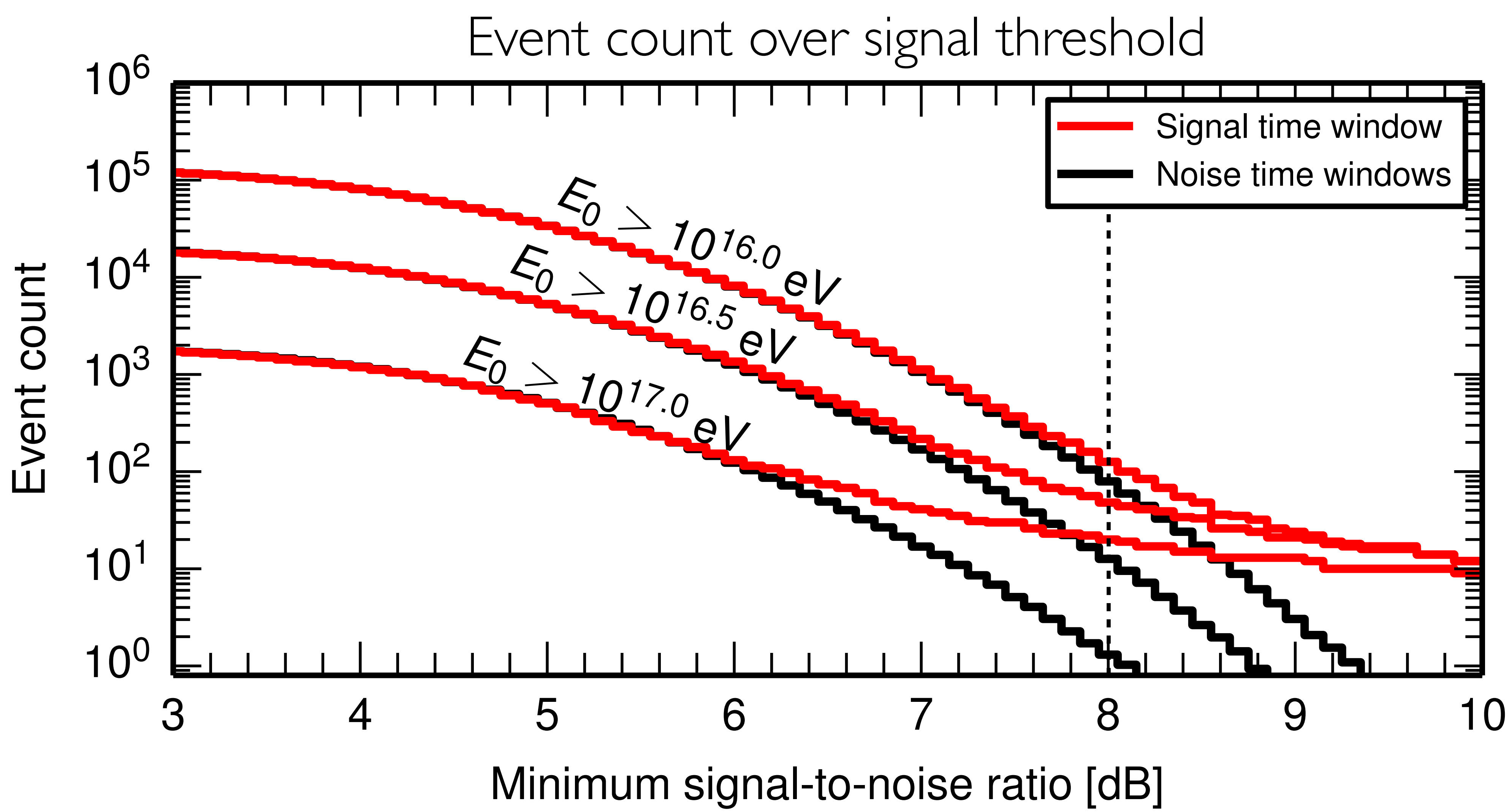

Events

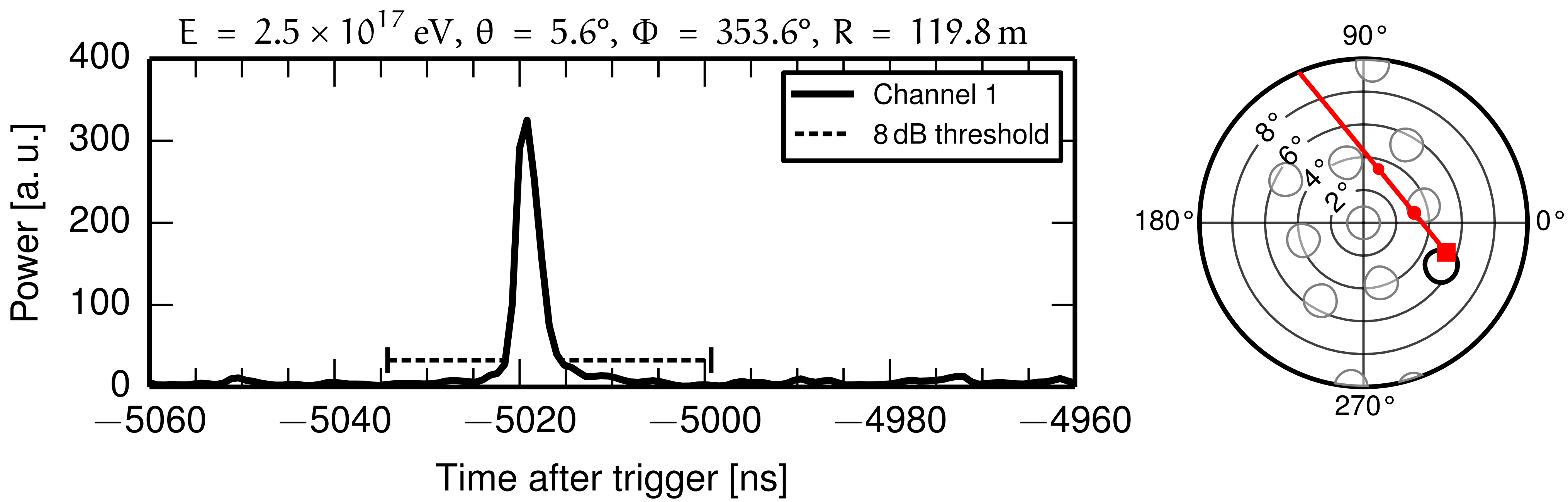

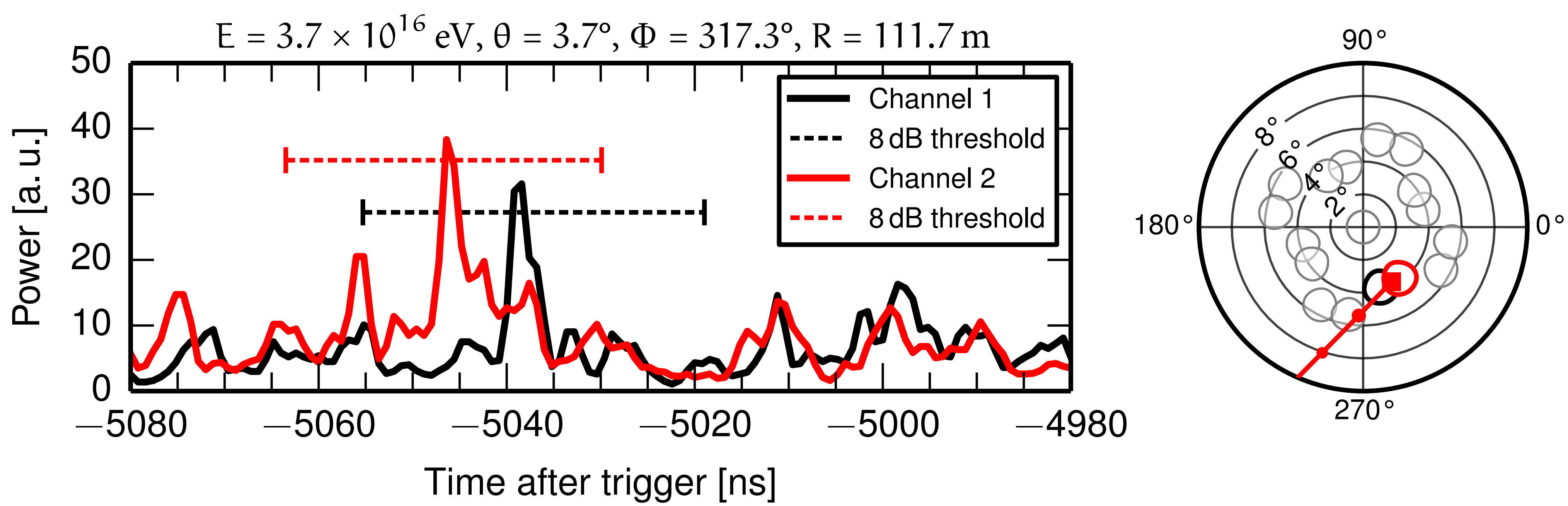

Common properties:

- short pulses (~5 ns)
- mostly single-receiver (only two stereo events)
- emission seems forward-directed
- signals originate from >2 km

Splitting the dataset

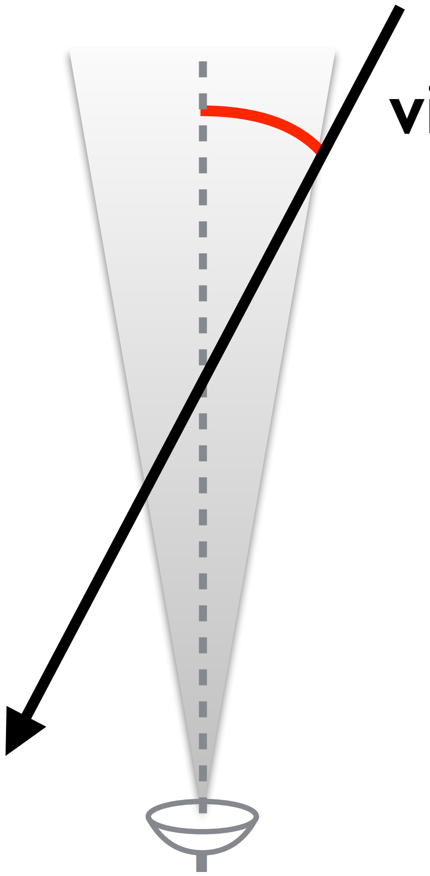

viewing angle: ∡(channel boresight, shower axis)

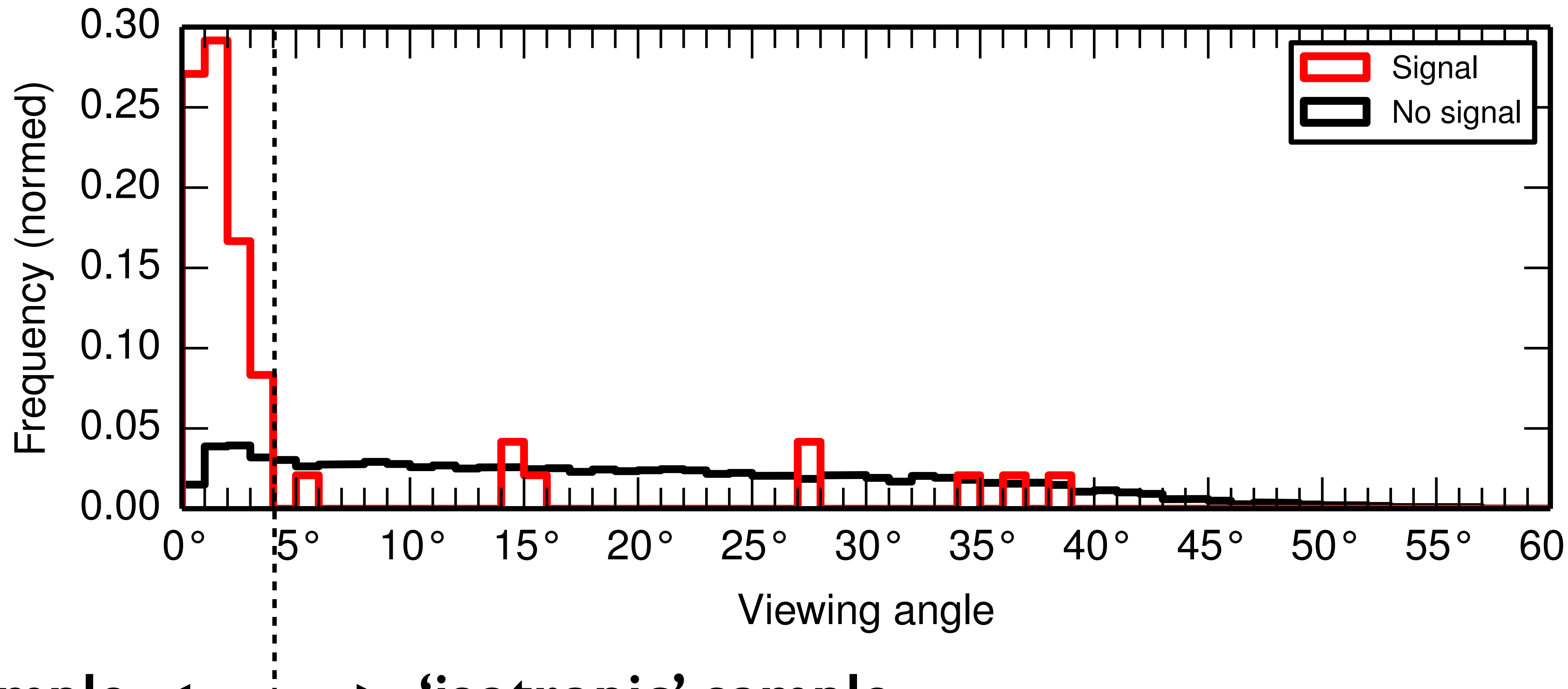

‘forward’ sample
39 signals
exp. <4 noise (95% C.L.)

‘isotropic’ sample
9 signals
exp. 11 noise

- 4° cut is compatible with Cherenkov angle at X_{max} + uncertainties
- most signals are detected in the forward region of the air showers
- isotropic sample is compatible with noise fluctuations

Forward region: Core positions

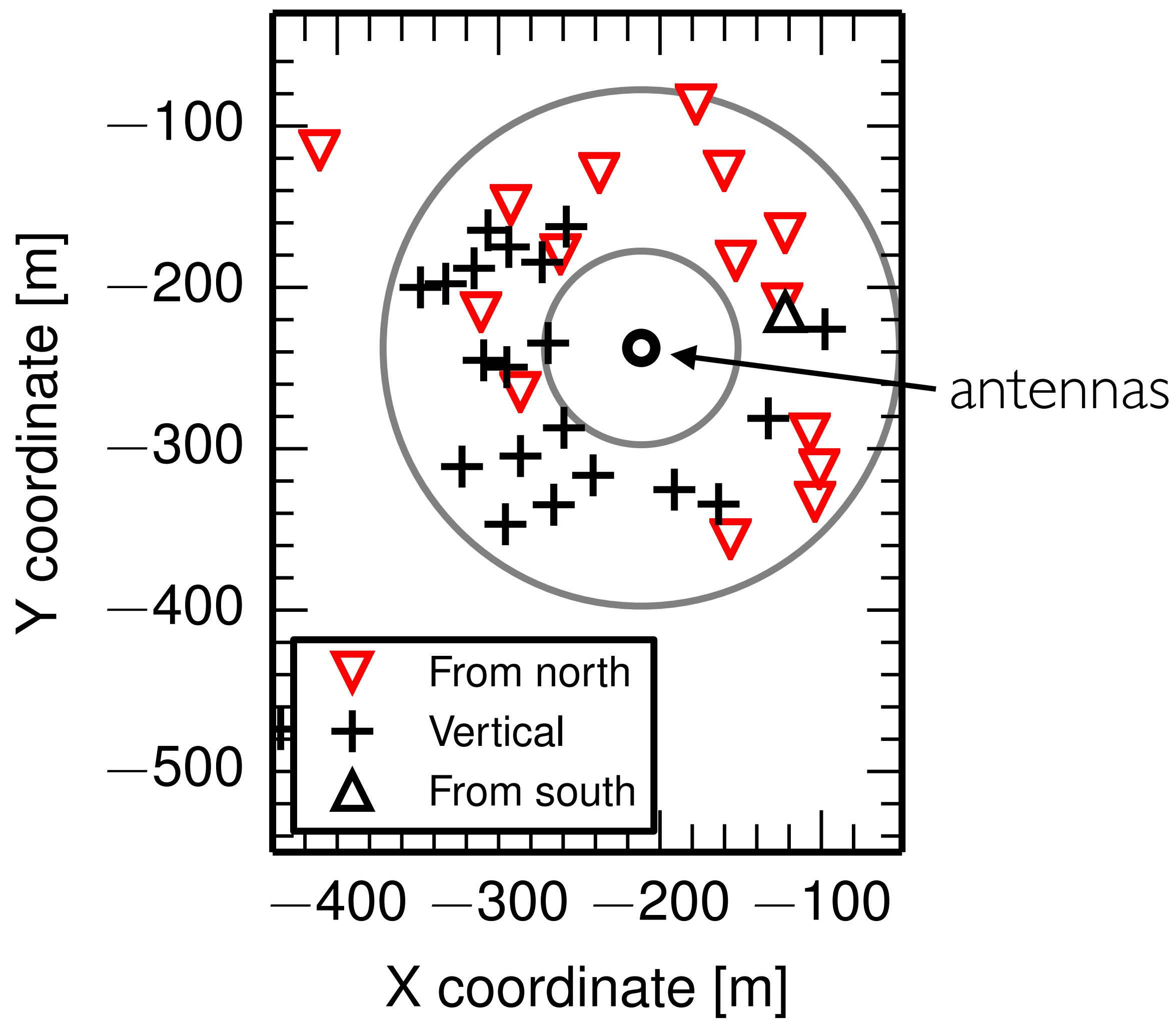

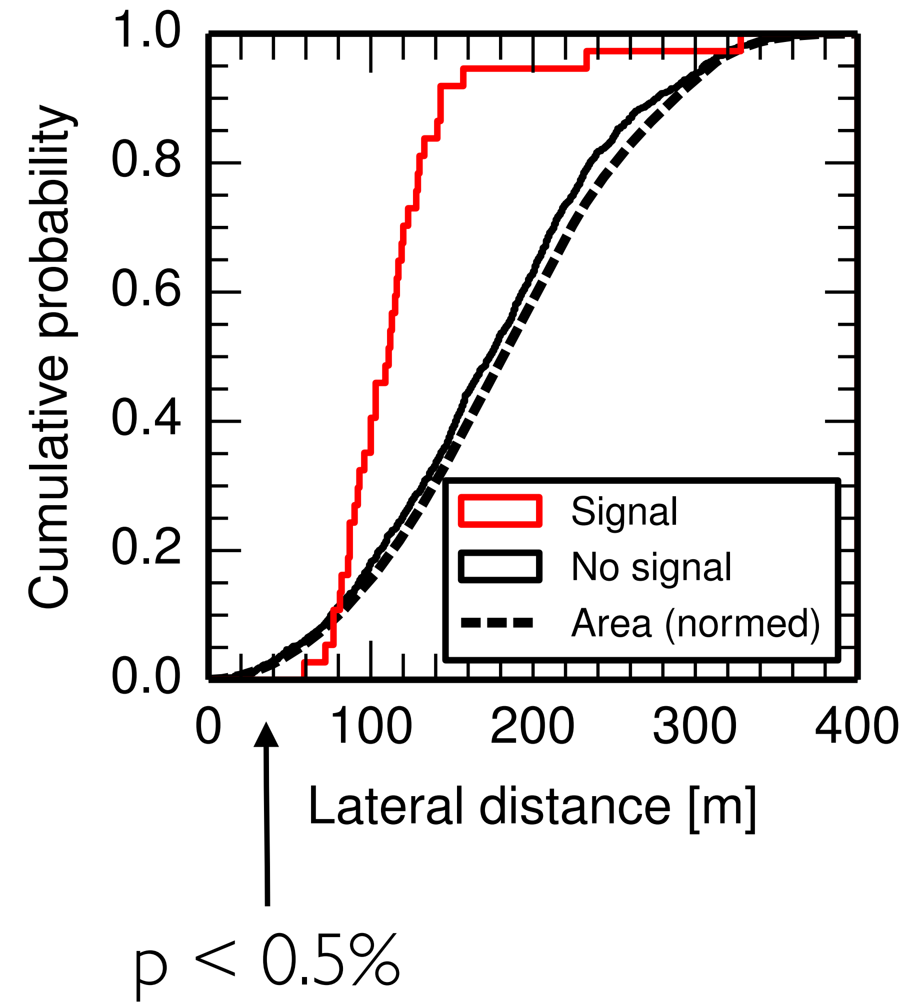

- clear **ring structure** (the two outliers vanish for 9 dB threshold)
- indication for **east-west asymmetry** in vertical antenna
- no asymmetry in north pointing antenna

Forward region: Arrival directions

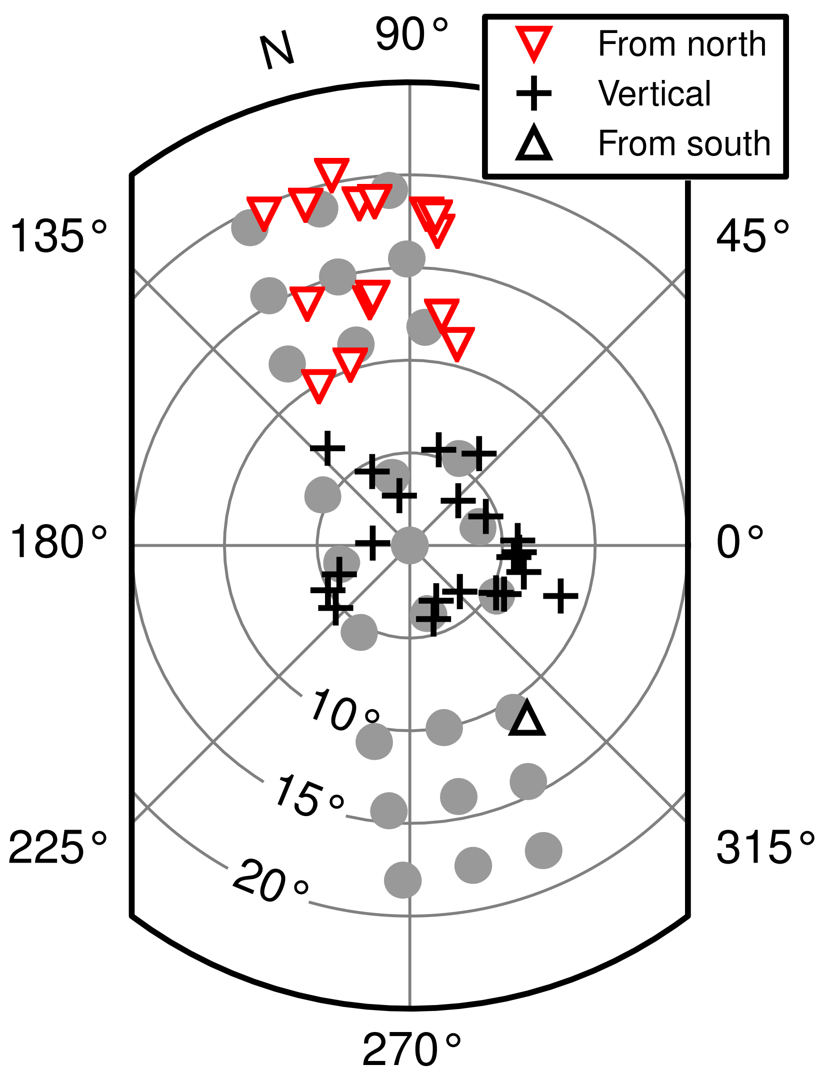

$\alpha_{mag} = 40°$ ‣ 9%

$\alpha_{mag} = 25°$ ‣ 7%

$\alpha_{mag} = 10°$ ‣ 1%

- indication that the detection rate increases with geomagnetic angle

Qualitative agreement with expectations from geomagnetic & charge-excess radiation

Forward region: Simulation of emission

Employ CoREAS (endpoint formalism; *cf.* J. Alvarez-Muñiz' overview):

T. Huege, M. Ludwig, and C.W. James. AIP Conf. Proc., 1535(1):128–132, 2013.

- simulate 25 proton and 25 iron showers with their parameters varied within the reconstruction uncertainties
- notable differences to typical VHF simulations:
  - 10^{-7} thinning
  - $\Delta t = 5$ ps ($f_{nyq} = 100$ GHz)
- add thermal noise and apply end-to-end electronics simulation
- **caveat:** use peak antenna gain
  - predicted signals should be treated as **upper limits**

10^{17} eV iron primary
(3.4–4.0 GHz)

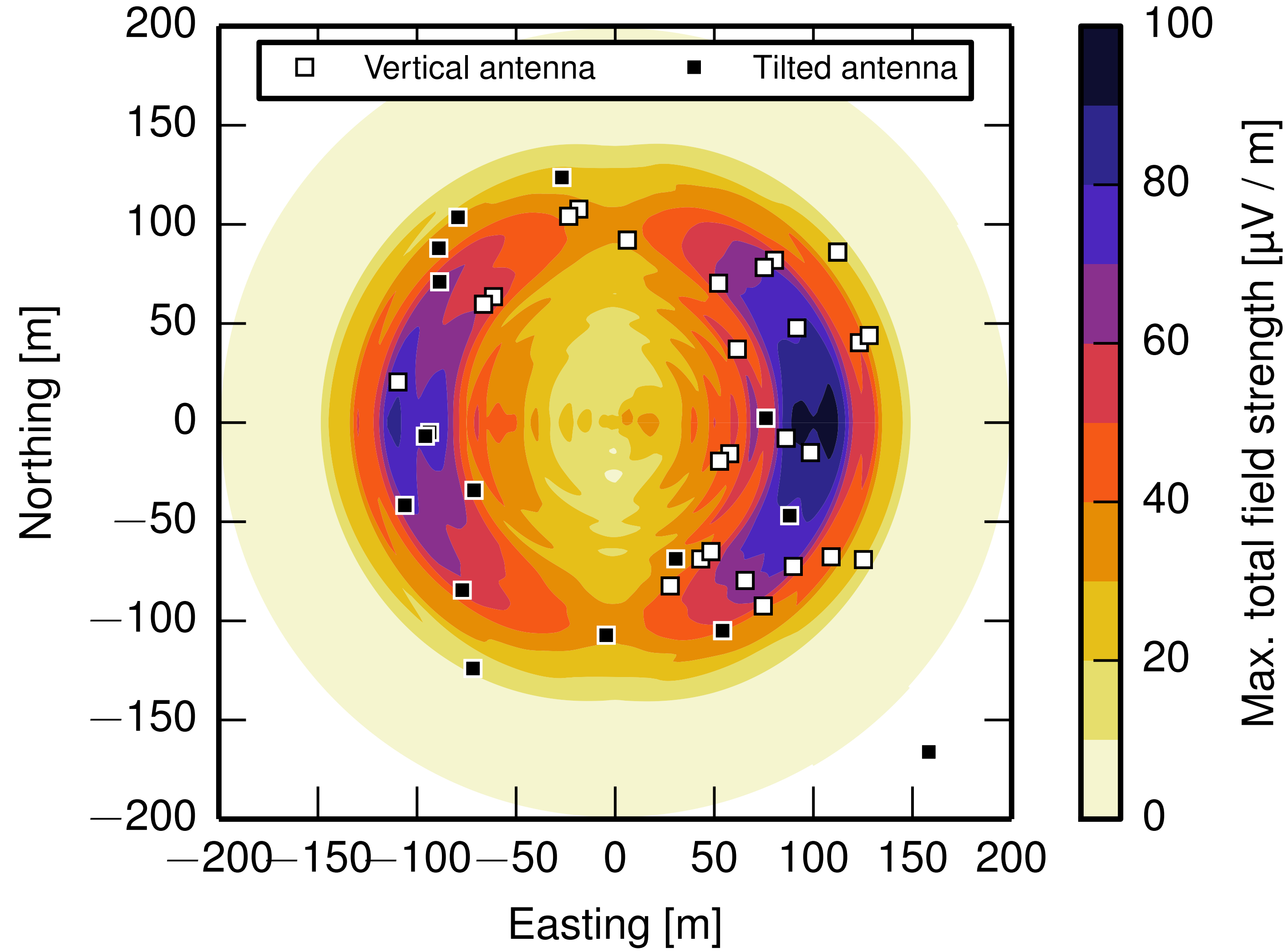

CoREAS: Comparison of polarisation pattern

- logamp detector destroys phase information
  - only **indirect** comparison of predicted signals with polarisation axes of receivers
- calculate **polarisation loss factor** (PLF) for each channel in the forward region of the detected events

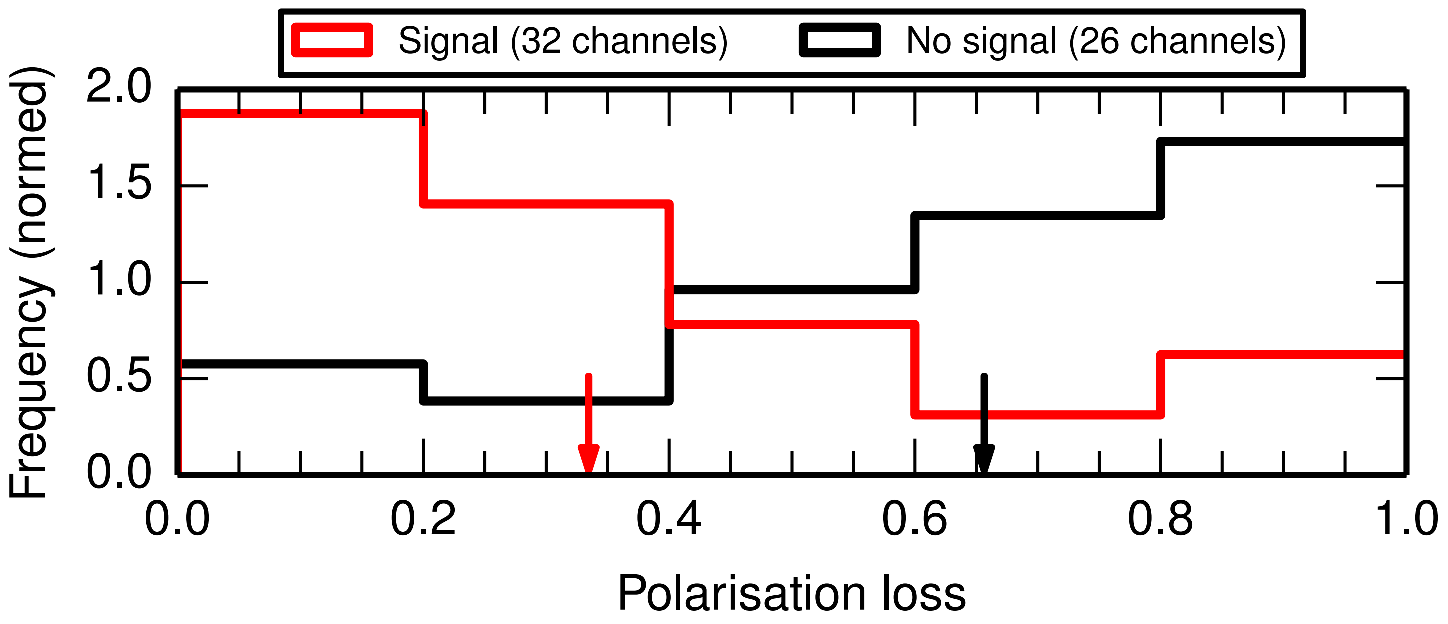

- detecting channels are well aligned with the CoREAS predictions
- dual-polarised measurements support this well
- distributions are incompatible with unpolarised radiation at 4.7σ level

CoREAS: Comparison of signal strengths

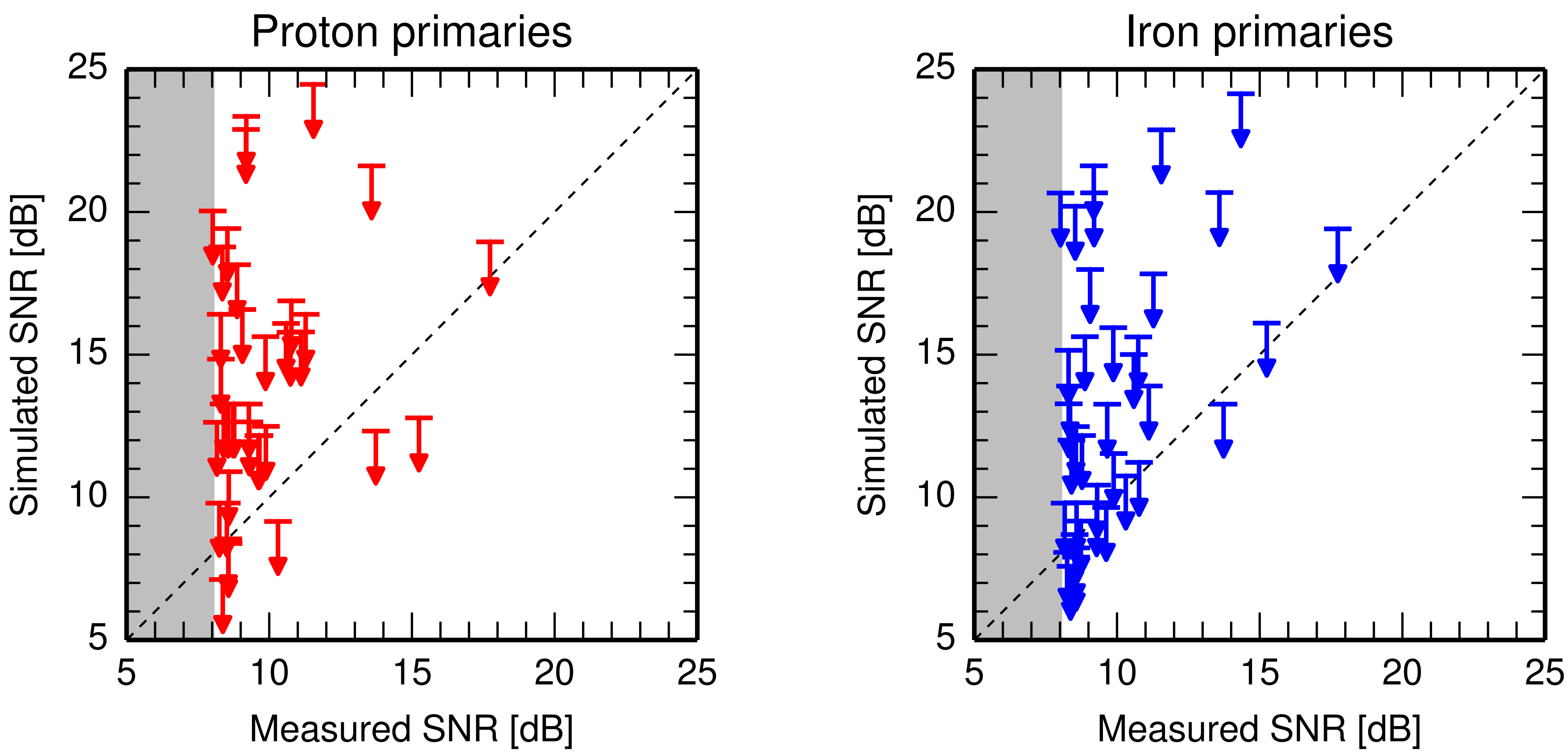

- overall **compatible** signal strengths
- showers with large discrepancies are generally farther from boresight
- data slightly **favours heavy primaries** (consistent with KASCADE-Grande data)

Isotropic sample: Simulation of emission

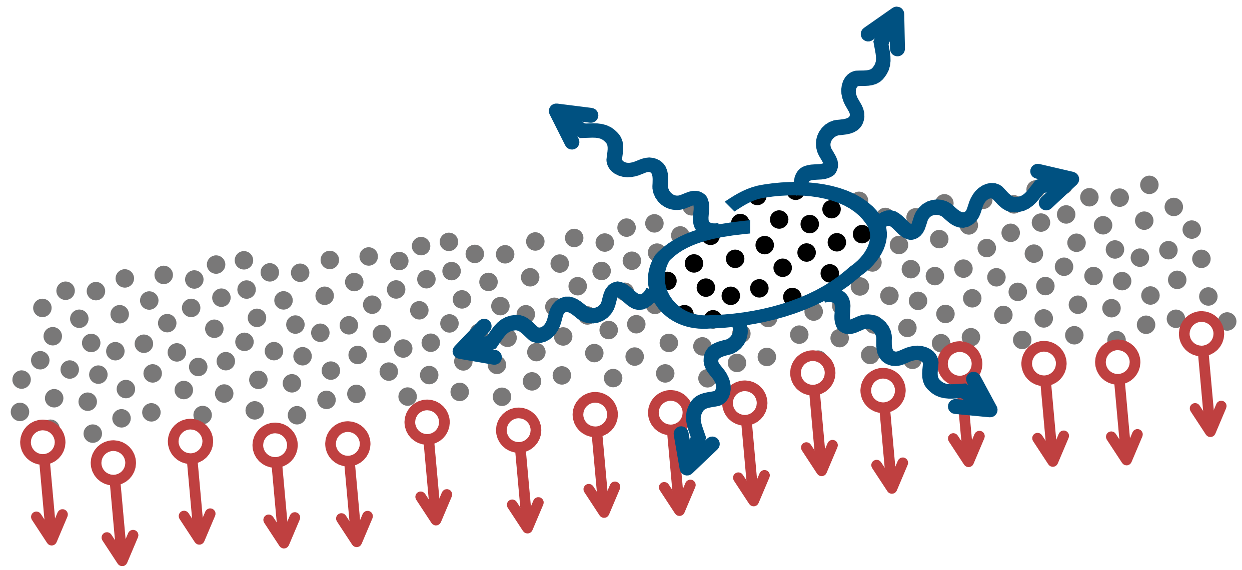

3-d Monte-Carlo based on shower parametrisations:

F. Nerling, J. Blümer, R. Engel, and M. Risse. Astroparticle Physics, 24(6):421–437, 2006.
L. Perrone, S. Petrera, and F. Salamida. Auger technical note GAP-2005-087, 2005.
D. Góra, R. Engel, D. Heck, et al. Astroparticle Physics, 24(6):484–494, 2006.

- emitted power proportional to energy deposit in atmosphere (linear scaling)
  - **microwave yield** of

    $$Y_{MW} = 1.2 \times 10^{-18}\ \mathrm{Hz}^{-1}$$

    reproduces accelerator measurements
- **flat spectrum** in C band; **unpolarised** and **isotropic**
- propagation to detector with height-dependent refractive index
- convolution with radiation patterns

MBR: Example of expected signals

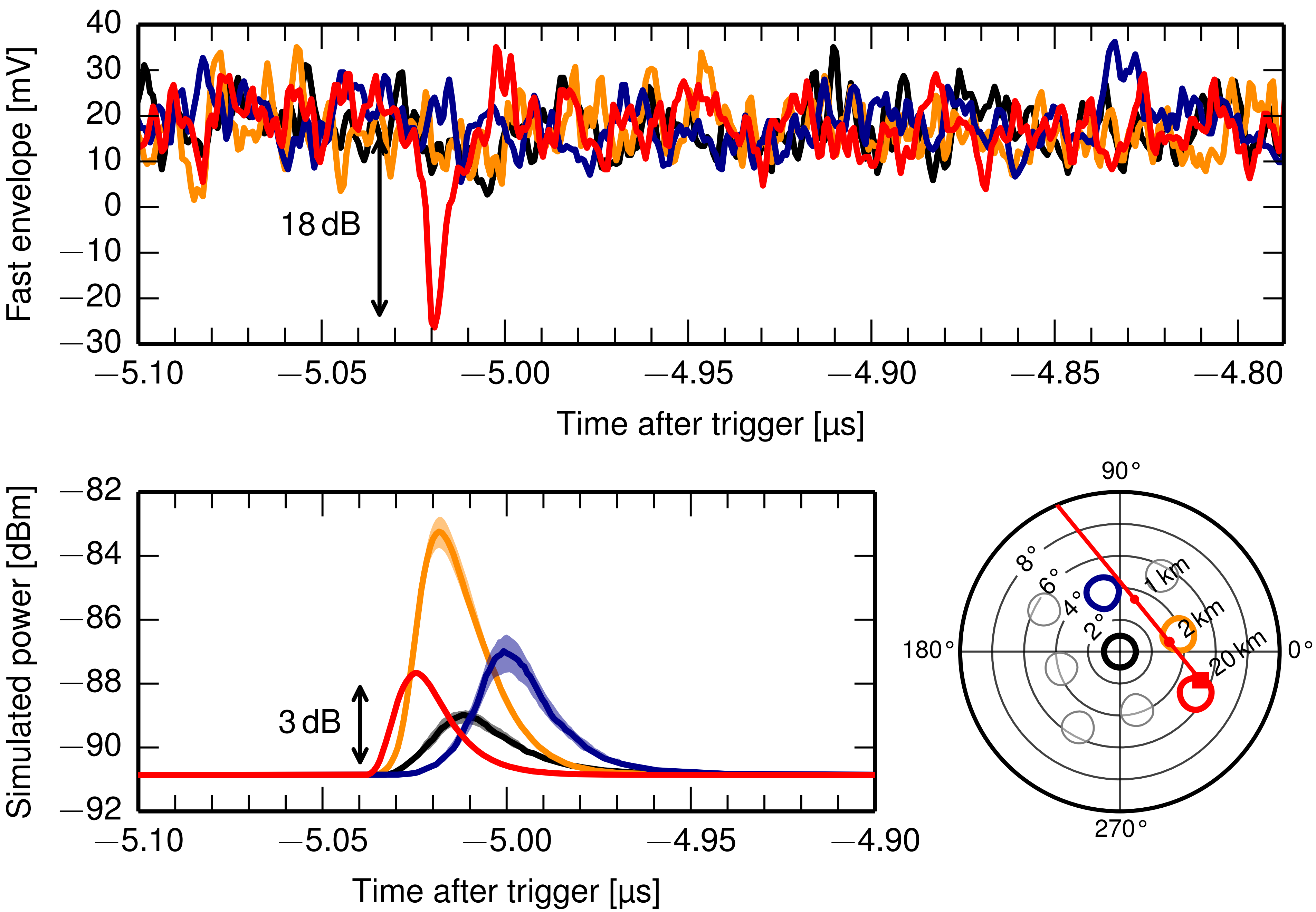

- isotropic model alone doesn't describe the spatial structure of the data

MBR: Comparison of signal strengths

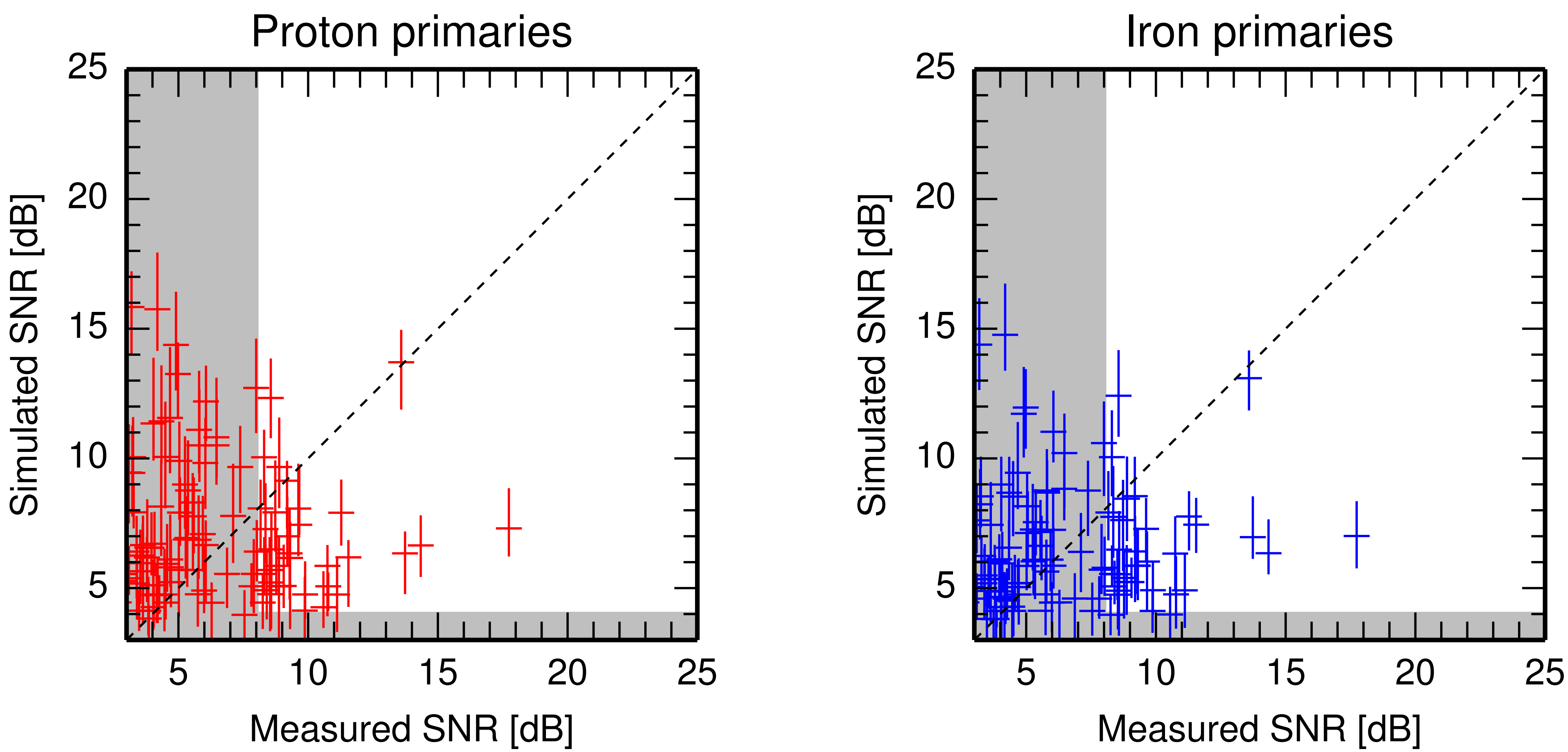

- **note:** all points with SNR_{data} > 8 dB have a viewing angle < 4°
- clearly **inconsistent** description of data (independent of rescaling)
  - since measurements are compatible with noise, derive **limit** on isotropic flux

Limit on isotropic, unpolarised component

Example for one channel

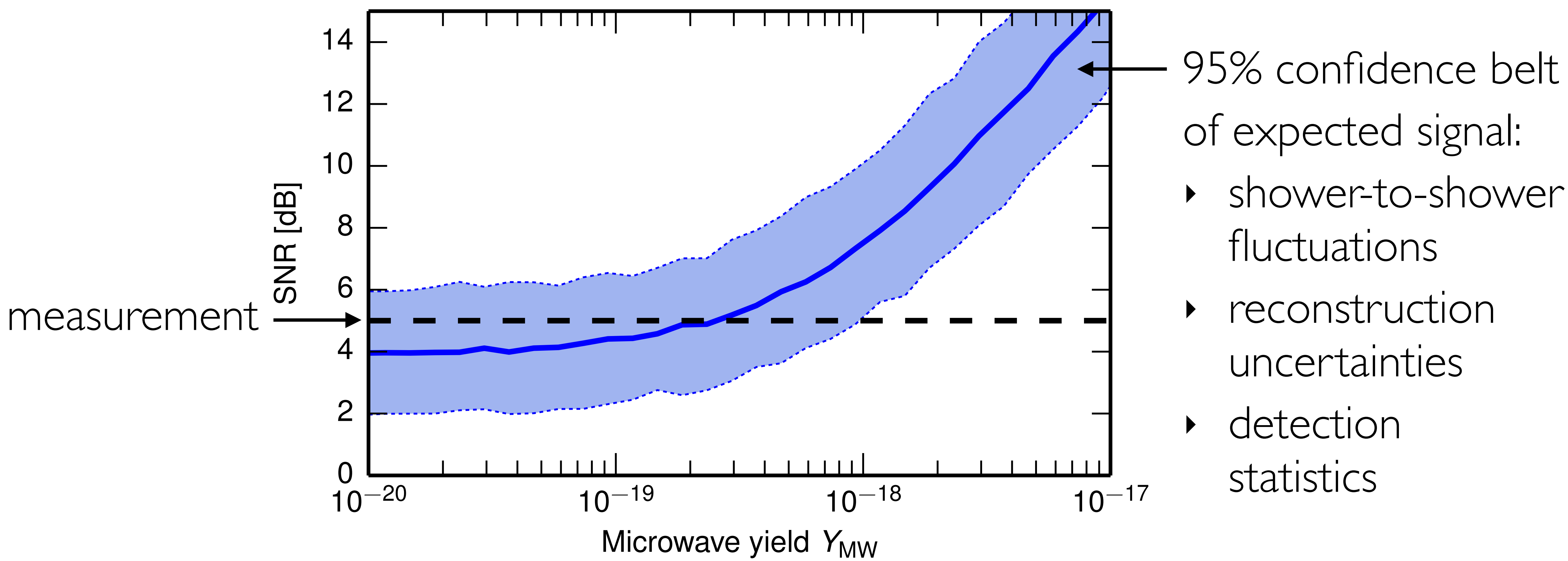

Combination of 'many' channels in a likelihood analysis:

$Y_{MW} < 0.4 \times 10^{-18}\ \mathrm{Hz}^{-1}$ (95% C.L., *preliminary*)

Conclusions on the microwave emission of EAS

Forward region:

- **fully consistent** description assuming geomagnetic and charge-excess as **sole** emission processes
- CoREAS predictions are compatible with measured polarisation patterns and signal strengths
  - still need to convolve simulations with antenna radiation patterns

Isotropic sample:

- measurements are compatible with noise
- **preliminary limit** on microwave yield of $Y_{MW} < 0.4 \times 10^{-18}\ \mathrm{Hz}^{-1}$ (95% C.L.)
  - in line with recent beam test experiments *(see, e.g., V. Verzi's talk)*
  - need to include more data and see how the limit evolves

Backup slides

Sensitivity for X_{max}

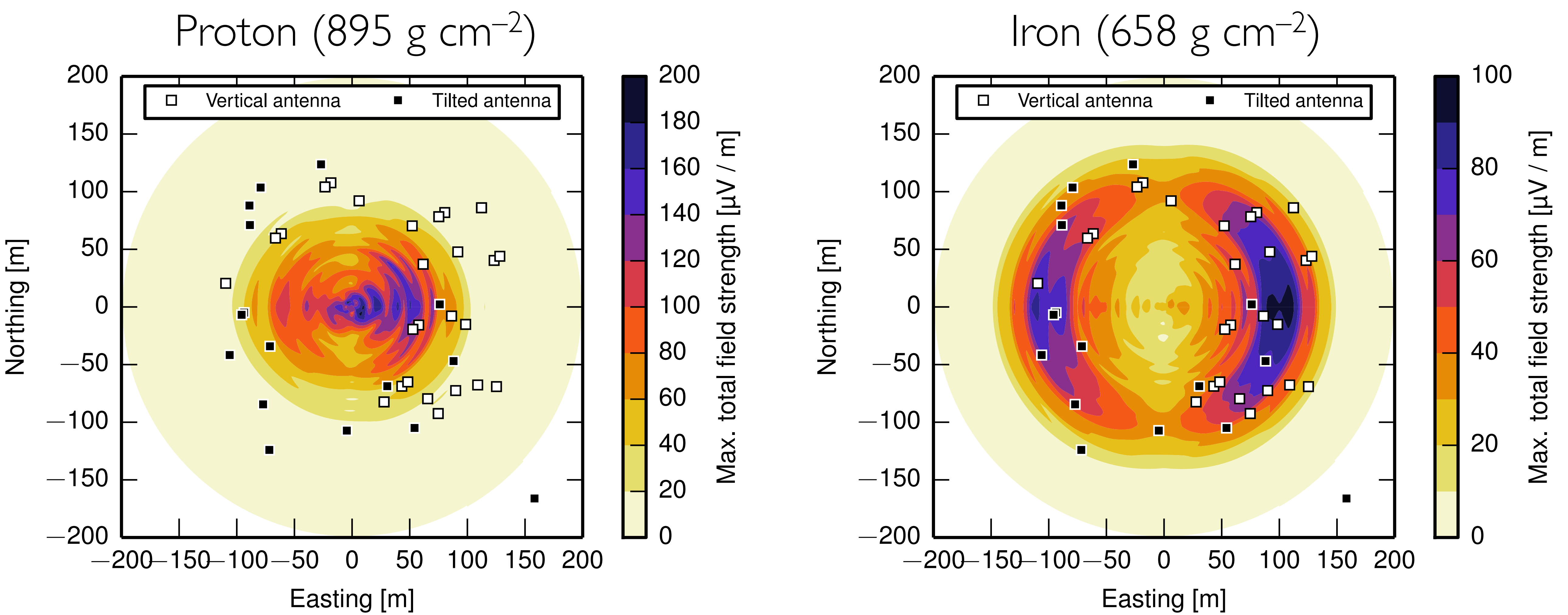

Polarisation map

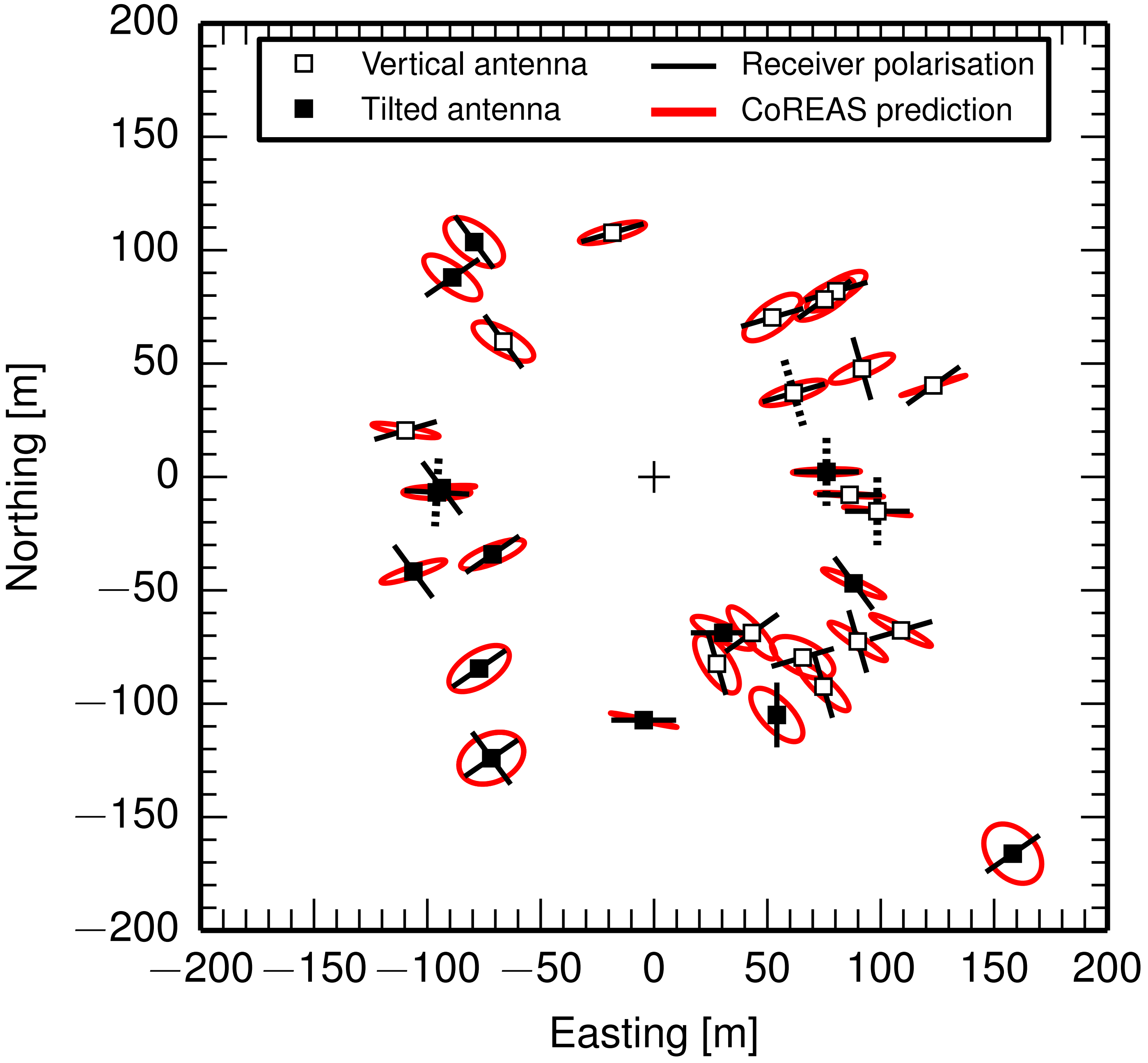

Event #851

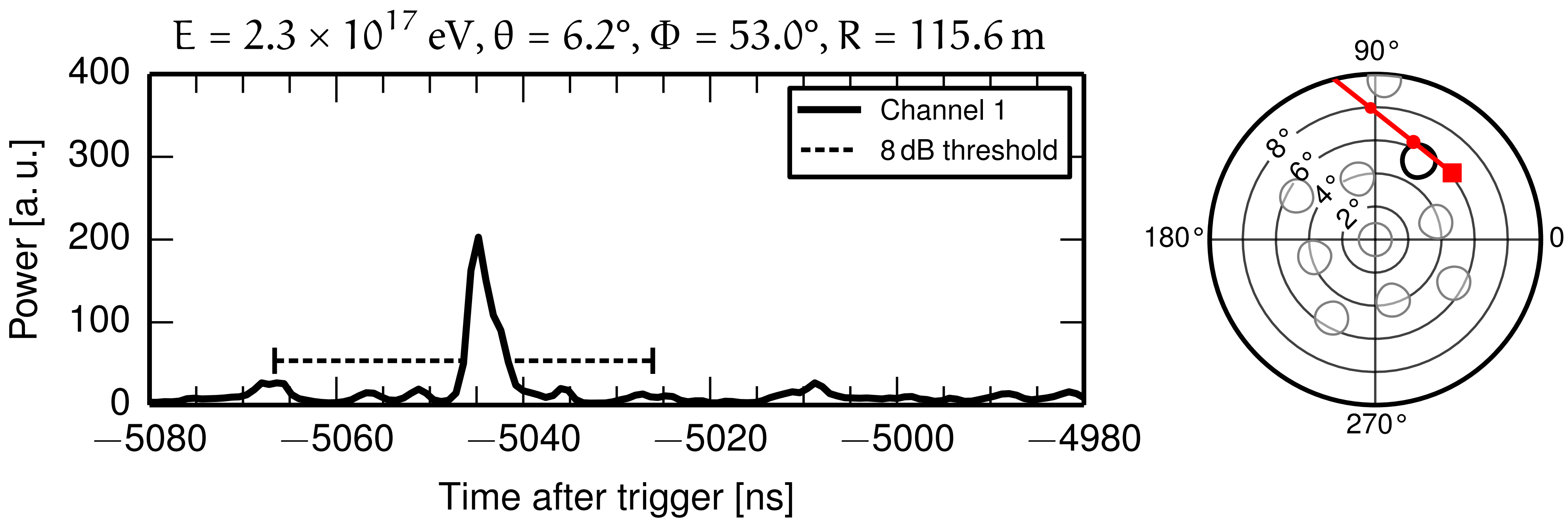

- MBR simulation fits well to **this** measurement
- however: channels in second antenna have similar predictions and **no** signals!

Dual-polarised measurement

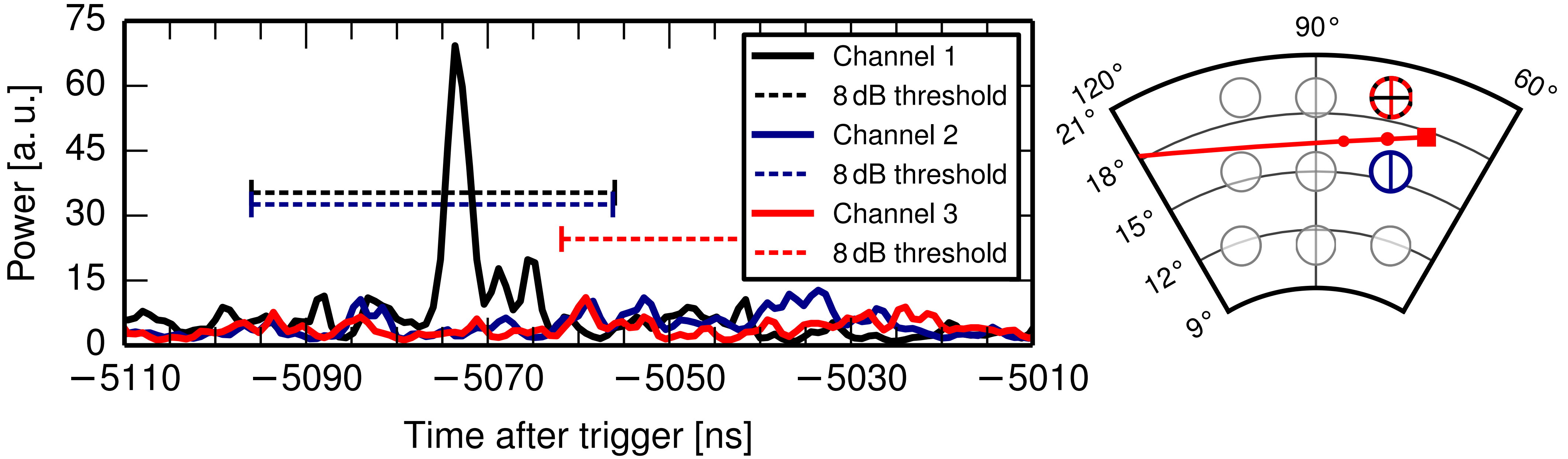

Rejection of noise events

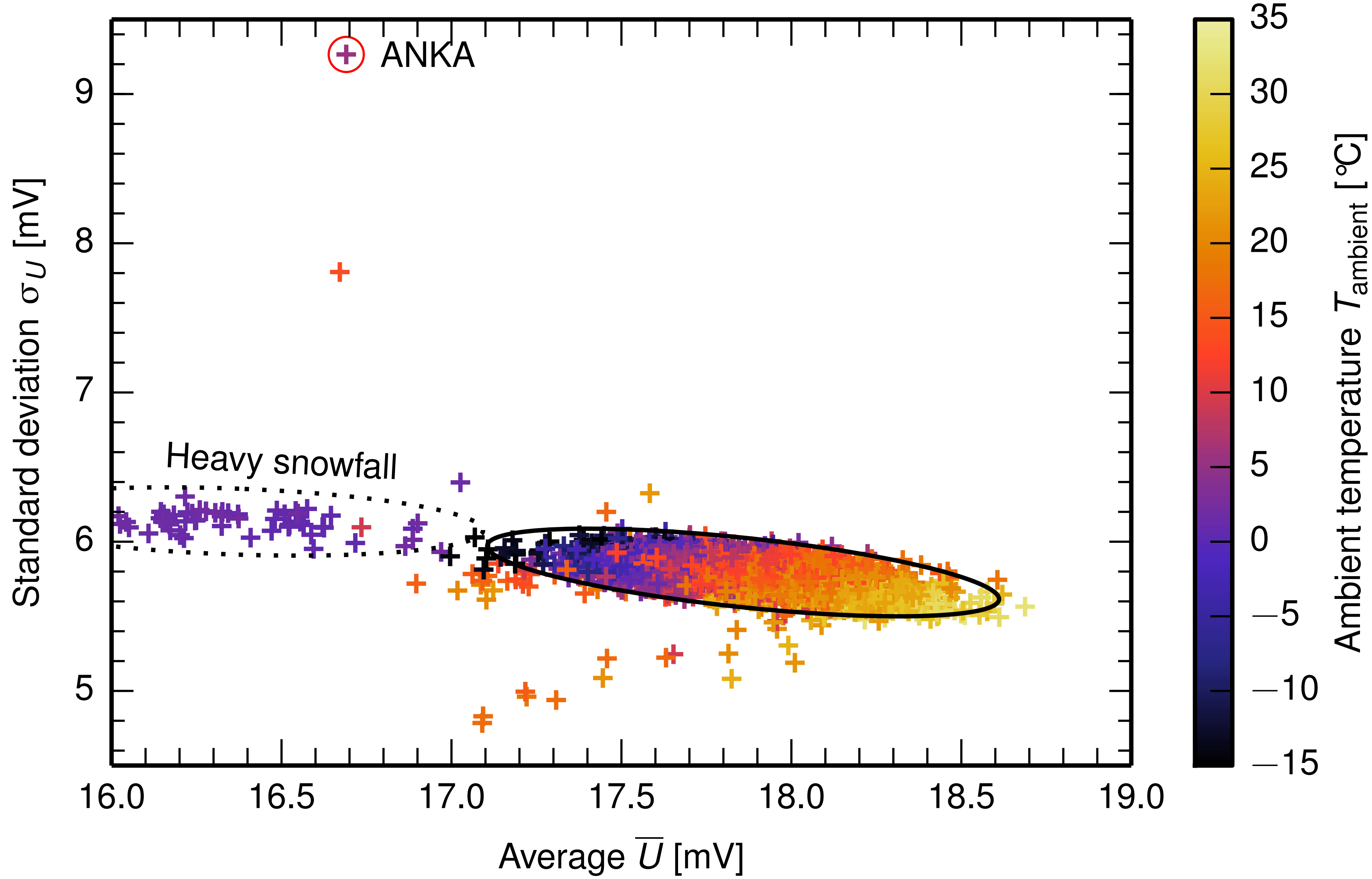

Uncertainty of impact time

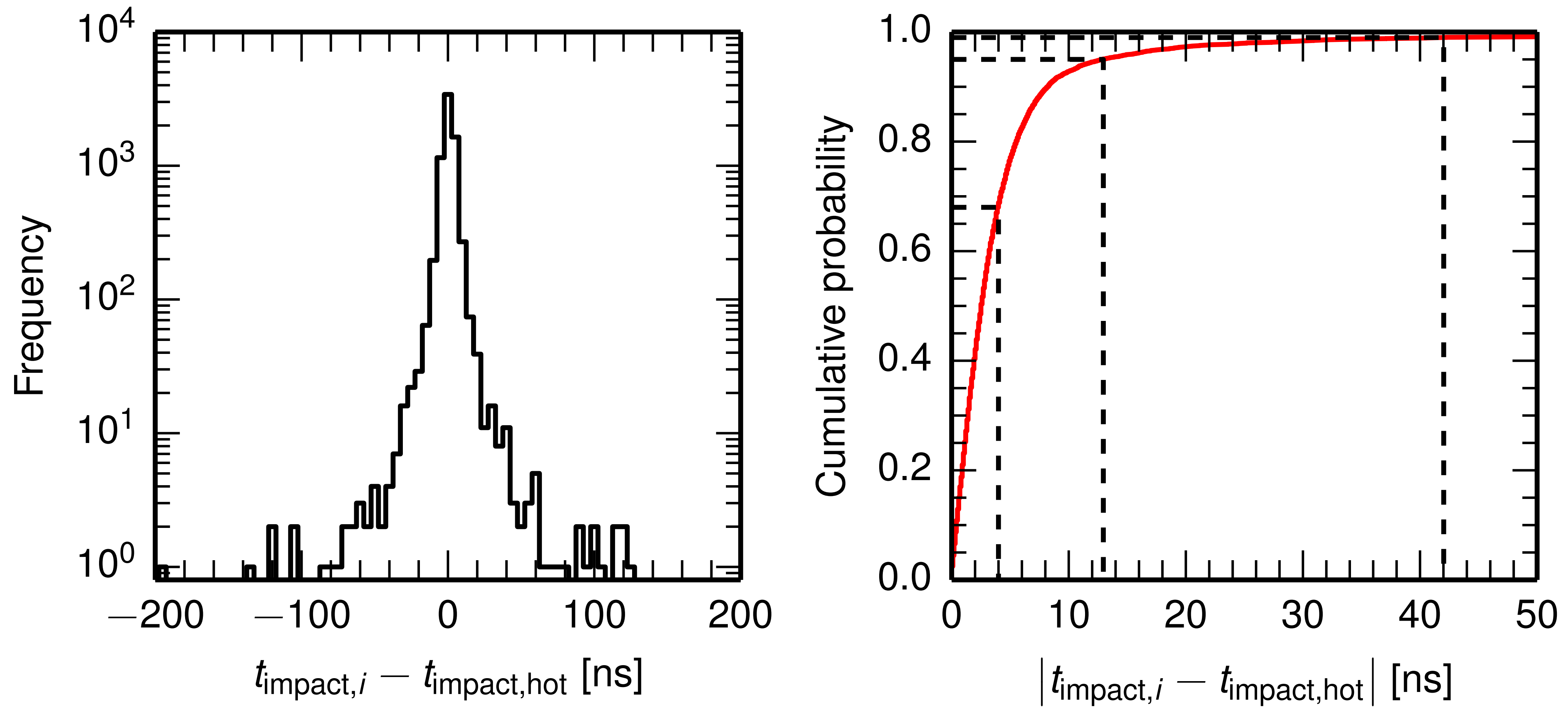

Stability of data taking